Published in final edited form as:
Gynecol Oncol. 2009 August ; 114(2): 188–194. doi:10.1016/j.ygyno.2009.05.014.

Laparoscopic optical coherence tomography imaging of human ovarian cancer

Lida P. Hariri[1], **Garret T. Bonnema**[2], **Kathy Schmidt**[3], **Amy M. Winkler**[2], **Vrushali Korde**[2], **Kenneth D. Hatch**[3], **John R. Davis**[4], **Molly A. Brewer**[1,5], and **Jennifer K. Barton**[1,a]

[1] Department of Biomedical Engineering, The University of Arizona, Tucson, AZ 85721-0104

[2] College of Optical Sciences, The University of Arizona, Tucson, AZ 85724

[3] Department of Obstetrics and Gynecology, The University of Arizona, College of Medicine, Tucson, AZ 85724

[4] Department of Pathology, The University of Arizona, College of Medicine, Tucson, AZ 85724-5043

[5] Division of Gynecologic Oncology, Carol and Ray Neag Comprehensive Cancer Center, The University of Connecticut, Farmington, CT 06030-2875

Abstract

Objectives—Ovarian cancer is the fourth leading cause of cancer-related death among women in the US largely due to late detection secondary to unreliable symptomology and screening tools without adequate resolution. Optical coherence tomography (OCT) is a recently emerging imaging modality with promise in ovarian cancer diagnostics, providing non-destructive subsurface imaging at imaging depths up to 2 mm with near-histological grade resolution (10–20 μm). In this study, we developed the first ever laparoscopic OCT (LOCT) device, evaluated the safety and feasibility of LOCT, and characterized the microstructural features of human ovaries *in vivo*.

Methods—A custom LOCT device was fabricated specifically for laparoscopic imaging of the ovaries in patients undergoing oophorectomy. OCT images were compared with histopathology to identify preliminary architectural imaging features of normal and pathologic ovarian tissue.

Results—Thirty ovaries in 17 primarily peri or post-menopausal women were successfully imaged with LOCT: 16 normal, 5 endometriosis, 3 serous cystadenoma, and 4 adenocarcinoma. Preliminary imaging features developed for each category reveal qualitative differences in the homogeneous character of normal post-menopausal ovary, the ability to image small subsurface inclusion cysts, and distinguishable features for endometriosis, cystadenoma, and adenocarcinoma.

Conclusions—We present the development and successful implementation of the first laparoscopic OCT probe. Comparison of OCT images and corresponding histopathology allowed for the description of preliminary microstructural features for normal ovary, endometriosis, and benign and malignant surface epithelial neoplasms. These results support the potential of OCT both as a diagnostic tool and imaging modality for further evaluation of ovarian cancer pathogenesis.

[a]To whom correspondence and reprint requests should be addressed: The University of Arizona, Department of Biomedical Engineering, 1657 E Helen Street #124, Tucson, AZ 85719. barton@email.arizona.edu. Voice: 520-626-8175, Fax: 520-626-8726.

Conflict of Interest statement:
The authors declare that there are no conflicts of interest.

Keywords

ovarian imaging; optical coherence tomography; laparoscopy; endoscopy; ovarian cancer; endometriosis

Introduction

Ovarian cancer is the most lethal of all gynecological cancer, partially attributed to a lack of distinctive early symptom manifestation and screening tests with adequate resolution and specificity. As a result, ovarian cancer is often diagnosed at advanced stages, after invasion of adjacent structures or metastasis to a distant site. Women with regional and distant disease have a 5-year survival rate of 71% and 30% (at best), respectively. If diagnosed at the localized stage, the 5-year survival rate is 92%; however, only about 19% of all cases are detected at this stage, typically identified incidentally during another medical procedure [1].

Currently, routine screening for asymptomatic women without an elevated risk for ovarian cancer is not recommended because screening tests with sufficient resolution are not available to date; the pelvic exam is the sole avenue for detection for women of average risk, occasionally aiding in the identification of disease which has often progressed to the more advanced stages. In women at high risk of ovarian cancer based on their personal or family history of other cancers, screening includes a combination of the pelvic exam, transvaginal ultrasound, and blood tests for tumor marker CA125 [1]. However, the sensitivity and specificity of these screening tools even in combination have been described as insufficient [2–6].

Ovarian neoplasms are classified based on their origination from surface epithelium, germ cell, or stromal tissue, with the vast majority of malignant neoplasms arising from the epithelium [7]. The current hypothesis in epithelial ovarian cancer pathogenesis is that ovarian neoplasms can be divided into two types [8]. Type I neoplasms (including low-grade micropapillary serous carcinoma, mucinous, endometrioid, and clear cell carcinomas) consist of slow growing neoplasms often confined to the ovary at diagnosis and develop from well-established precursor lesions. Type II neoplasms are aggressive, rapidly growing neoplasms thought to arise from surface epithelium or subsurface epithelial inclusion cysts, including high-grade serous carcinoma [8]. Conventional white light laparoscopy allows for the identification of larger surface abnormalities, but does not provide subsurface information and thus may not be capable of visualizing the earlier stages of Type II neoplasms. The ability to visualize lesions not grossly visible and/or subsurface lesions either laparoscopically or transvaginally may potentially improve diagnostic capabilities for these more aggressive Type II lesions.

Optical coherence tomography is a recently emerging non-destructive imaging technology, using a near-infrared broad-bandwidth light source to achieve subsurface imaging with high axial resolution (10–20 microns) at imaging depths up to 2 mm. Contrast is generated from light backscattered from index of refraction mismatches to create high-resolution cross-sectional images without requiring application of exogenous dyes. OCT can be adapted for fiber based endoscopic applications with relative ease, including miniaturization for small diameter applications, and has been evaluated in a wide array of *in vivo* applications, including human eye [9,10], gastrointestinal tract [11,12], and coronary artery [13,14].

OCT has also been used to study the structural features of gynecological tissues, including *ex vivo* ovary [15–17], *in vivo* ovary during laparoscopy [18], and endometrium and uterine cervix [16,18–24]. Previously, we studied *ex vivo* OCT imaging in normal and diseased

human ovary and found OCT capable of resolving tissue level changes, including inclusion cysts, endometrial implants, and superficial tumor masses. Changes in stromal organization and directionality of collagen fibers thought to be associated with malignancy were suggested in several of the images of cancer. Areas of necrosis and blood vessels were also visualized, which were indicative of an underlying abnormality in the tissue [17].

We recently developed the first custom laparoscopic OCT device fabricated specifically for laparoscopic procedures. In this study, we utilized laparoscopic OCT to image the ovaries of patients undergoing oophorectomy to determine the feasibility and safety of laparoscopic OCT imaging and evaluate the tissue microstructural features of ovarian tissue *in vivo*.

Materials and Methods

Patients

Patients undergoing exploratory laparotomy or transabdominal endoscopy and oophorectomy at University Medical Center at the Arizona Health Sciences Center of the University of Arizona in Tucson were asked to participate in this *in vivo* imaging study. Patients were excluded from the study if they were under 18 years of age or pregnant. The study was approved by the Institutional Review Board of the University of Arizona and informed consent was obtained from each patient who participated.

Laparoscopic OCT

The OCT system uses a superluminescent diode light source with a 1300 nm center wavelength and a full-width half-maximum bandwidth of 100 nm (SuperLum D1300-HP, Moscow, Russia), providing a measured axial resolution of 11 μm in air. The source light was split into two fibers using a 2×2 coupler, one leading to a reference mirror and the second to the laparoscopic probe that focused light on the tissue. The power on the sample was measured to be 1.5 mW. Light reflected from the reference mirror and backscattered by the sample were recombined within the 2×2 coupler. When the optical path length difference between light in the sample and reference arms was within a coherence length of the source (approximately 14 μm), interference was observed. The reference arm pathlength was modulated with the use of a rapid scanning optical delay line [25]. The interferometric signal was detected using a photodiode (Optiphase Model V500, Van Nuys, California) and detector output was demodulated to obtain a signal envelope proportional to the magnitude of backscattered light within the sample. A single depth-resolved line of data is referred to as an a-scan and a series of a-scans were collected to form a two dimensional depth-resolved image of the tissue. This setup was capable of producing a-scan rates from 100 to 1000 a-scans/s. The signal was acquired and processed using custom C# software with a high-speed National Instruments data acquisition board (PCI-6111, National Instruments, Austin, Texas).

The sample arm of the interferometer was the laparoscopic OCT probe containing an OCT channel single-mode fiber. Light in the OCT channel was focused by a gradient-index (GRIN) lens, producing an axial resolution of 11 μm and lateral resolution of approximately 25 μm at a working distance of 300 μm. A standard 45-degree angle rod prism was used to direct the light out of the side of the probe. The OCT fiber and endoscopic optics, such as the GRIN lens and rod prism, were housed within a 2 mm inner diameter, 28 cm long stainless steel sheath (Small Parts, Miramar, Florida) with the rod prism exposed at the distal end of the inner sheath. The inner sheath was housed inside of a removable, sterilizable outer sheath, consisting of a distally sealed 4 mm outer diameter (OD) 100% Pyrex glass tube adhered inside of a 4.6 mm OD, 29 cm long stainless steel tube (Small Parts, Miramar, Florida). A 180° 16 mm long window was cut into the outer stainless steel tube, exposing

the Pyrex glass and creating an imaging window for the side-directed light to pass. A micro-miniature positioning stage (Del-Tron Precision, Bethel, Connecticut) was used to linearly translate the optics. The motion was transferred to the inner sheath, while the imaging window remained fixed in place by the outer sheath. The micro-miniature positioning stage and fiber connector were housed inside of a custom-built 3.8 cm OD cylindrical aluminum encasement.

Imaging Procedure

To maintain sterility, the entire outer lumen was sterilized following standard ethylene oxide sterilization protocols. The remainder of the laparoscopic OCT probe was enclosed by a 3Prime; × 96Prime; sterile ultrasound probe cover (Sheathing Technologies, Morgan Hill, CA), fastened with sterile elastic bands at the distal and proximal ends of the probe handpiece. Following exploratory laparotomy or transabdominal endoscopy, the laparoscopic OCT probe was inserted into a laparoscopic port by the surgeon (K.H.). The surgeon placed the imaging window in contact with ovary at a desired imaging location (Figure 1) and a 4.0 mm × 1.4 mm (800 × 1000 pixels) image was acquired at 1 mm/s. Up to four sites per ovary and one or both ovaries were imaged within a 5-minute time frame. Oophorectomy was performed subsequent to OCT imaging.

Pathology

Following oophorectomy, up to four biopsies (typically 4 mm × 2 mm × 1.5 mm) corresponding to OCT imaging sites were removed from each ovary when this did not impact pathological diagnostics (i.e. in specimens not needed for frozen section diagnosis). Following standard practice on clinical specimens, both gross and microscopic pathology was analyzed on the entire ovary. Biopsies were fixed, processed, stained with H&E by standard histological procedures, and reviewed by pathologists at the University Medical Center Pathology Department. In addition to biopsy sites, University Medical Center surgical pathology reports and specimen slides were obtained for each ovary imaged. If specimens were sent for frozen section diagnosis and biopsies were not obtainable, then pathology specimens and reports were used for histopathological confirmation.

OCT Image Analysis

OCT images were categorized into four categories based on histopathological diagnosis: 1) normal ovary (including normal ovarian stroma and benign cysts), 2) endometriosis, 3) cystadenoma, and 4) adenocarcinoma. Features observed in OCT images such as stromal changes, surface abnormalities, and presence of cysts, glandular structures, and increased vasculature were correlated with corresponding histopathology and utilized to develop preliminary features for the above categories.

Results

Thirty ovaries of seventeen patients (ages: 39–85 years, average age: 60.7 years) were imaged with laparoscopic OCT successfully during laparoscopy or laparotomy without any known complications. In four patients, only unilateral ovarian imaging was performed at the surgeon's discretion. Images from both ovaries of one patient were removed from analysis due to imaging artifacts precluding analysis of the data. Of the remaining twenty-eight ovaries, sixteen were diagnosed as normal (Figures 2a–b), five with endometriosis (Figure 3a–b), three as papillary serous cystadenoma (Figure 4a–b), and four as adenocarcinoma (two papillary serous cystadenocarcinoma and two endometrioid adenocarcinoma, Figure 4c–d). A summary of these results can be found in Table 1.

OCT data analysis

In OCT imaging of normal peri and post-menopausal ovaries (Figure 2), the single layer of epithelium covering the surface of the ovary is not within resolution of system. However, the boundary between the epithelial lining and underlying stroma, although thin, can be visualized as a bright backreflection when the boundary is perpendicular to the incident light, occurring intermittently within each image (arrow head, Figure 2a) probably due to being composed of mainly Type IV collagen. The appearance of normal ovarian stroma in OCT is relatively hyperintense, exhibiting a homogeneous, but distinctive texture mimicking the highly cellular, randomly oriented collagen fibers seen in the corresponding histopathology (labeled S, Figure 2a–b). The ovarian stroma is composed primarily of Type I collagen. Corpora albicans are frequent in post-menopausal ovaries and appear as signal void regions of variable size with poorly defined boundaries circumscribing the corpus albicans (labeled CA, Figure 2a–b). The lack of optical contrast resulting in the signal void region may be due to the acellular, degenerated collagenous content of the structure

Epithelial invaginations can be seen as variably sized signal void clefts along the epithelial surface with a sharp, well-defined lining. Similarly, epithelial inclusion cysts are visualized as variably sized, circumferential signal void regions within the ovarian stroma with a sharp, well-defined border, probably due to the Type IV collagen that is under the surface epithelial cells lining the inclusion cyst. In contrast, fluid filled benign cysts appear as homogeneously hypointense regions, with approximately two-fold more density than the inclusion cysts, and have the same well-defined borders. As our dataset consisted primarily of peri and postmenopausal patients, we did not image any follicular cysts.

Five of the ovaries imaged (two bilateral and one unilateral case) were diagnosed post-surgically with endometriosis (Figure 3). In OCT, endometriosis glands appear as variably sized implants on the ovarian surface or within the ovarian stroma. The implants consist of well-defined, homogeneously signal poor regions (relative to normal stroma) with mild underlying shadowing due to light attenuation from blood. Within the cases of endometriosis, there were 4 endometriomas (1.0–2.3 cm greatest diameter), which appear in OCT as a large, homogeneously signal poor mass. Additionally, increased numbers of large diameter vessels were seen at the surface of or superficial to the normal ovarian stroma (arrows, Figure 3a), as we also observed as histopathologic features of endometriosis (arrows, Figure 3b). These large diameter vessels are identified as signal poor bands or circles and display occasional underlying shadowing due to light attenuation from blood.

The papillary serous cystadenoma is characterized in OCT (Figure 4a) as a large, simple cystic structure with a sharp, regular, well-demarcated cyst lining. Surrounding the cystadenoma is a region of relative hyperintensity (as compared with normal ovarian stroma), containing large signal void circumferential structures casting a shadow over the underlying tissue structures. These features represent multiple large diameter vessels (arrows, Figure 4a–b) within the hypocellular stromal tissue adjacent to the cystadenoma. The cystadenoma (labeled C, Figure 4a–b) has a sharp and well-demarcated lining in the OCT image, which contrasts sharply with the images seen with endometriosis and cancer that have a poorly demarcated border probably due to invasion into the underlying stroma. Endometriosis represents a benign but invasive process while cancer represents a malignant invasive process.

Four cases of adenocarcinoma (two papillary serous and two endometrioid adenocarcinoma) were imaged in this study. For the purposes of identifying preliminary features of adenocarcinoma, the two types of adenocarcinoma were evaluated together. Generally, adenocarcinoma was visualized as a complex, multicystic signal void structure (labeled C, Figure 4c–d). In this case, the cancer arose within the ovary and not on the surface,

presumably within an inclusion cyst. This represents on one of the advantages of OCT over other optical imaging modalities in that it can penetrate to the depth where the majority of these cancers arise within an inclusion cyst. OCT imaging of cyst epithelial lining varied in appearance, appearing well-demarcated when the lining was single layered and poorly-defined when the lining was multi-layered or contained papillary excrescences. The single layered area was benign and identical to the pattern seen in the serous cystadenoma. Malignant epithelial papillations and glands were visualized as irregularly shaped, variably sized signal void spaces with poorly defined borders (circled region, Figure 4c–d). The stromal component encompassing the cystic mass and/or intervening between malignant glandular epithelium displayed considerably more heterogeneous signal intensity than normal ovarian stroma. Additionally, a linear feature in the stromal component was noted, appearing to approximate the parallel collagen fiber orientation seen in the histopathology of the malignant ovaries (labeled S, Figure 4c–d) rather than the random fiber orientation of the normal ovarian stroma. The stroma contained increased vasculature, consistently visualized as signal poor bands (longitudinal) or circles (if cross-sectional) with underlying shadowing due to light backscatter from red blood cells (arrows, Figure 4c–d). Areas of necrosis were visualized as heterogeneously signal poor to signal void regions with poorly defined borders.

Discussion

Laparoscopy provides a method of external visualization of the ovaries, but is limited to surface topography. OCT provides cross-sectional, depth-resolved information, providing the ability to interrogate tissues with micron-scale resolution without destruction or required excision of the tissue. We present the development of the first OCT probe fabricated specifically for laparoscopic procedures. The successful implementation of laparoscopic OCT for *in vivo* human ovarian imaging demonstrated both its feasibility and safety. Comparison of OCT images to histopathology showed that OCT could evaluate microstructural features of normal ovary, endometriosis, and neoplasms of surface epithelium and the identified features are consistent with those described in previous *ex vivo* studies [15–17].

Post-menopausal ovarian stroma was visualized as a relatively hyperintense region with a homogeneous, but distinctive texture appearing to mimic the randomly oriented Type I collagen fibers of the normal stroma. This appearance and texture of the normal stroma can differentiate a normal postmenopausal ovary from ovarian pathology, such as endometriosis, cystadenoma, and adenocarcinoma.

The visualization of small epithelial invaginations and inclusions cysts with OCT is of particular importance given that these inclusion cysts are suspected to be the precursor lesions for aggressive Type II ovarian carcinomas [8]. The high resolution and subsurface imaging capabilities of OCT allow visualization of these inclusion cysts where they would likely be unidentifiable by laparoscopy alone and could be missed by histologic sections if the entire ovary was not embedded and sectioned. This may have an application in the management of women with a BRCA mutation who have a 4–17% risk of malignancy [26–28]. Although there have been numerous publications about the necessity of careful sectioning of the ovary and the tube, being able to visualize these areas in real time would be important in determining which women needed oophorectomy in pre-menopausal patients wishing to preserve fertility. Although we did not address the role of tubal cancers in the BRCA population, this technology could be easily adapted to the regular morphology of the fallopian tube. The ability to reliably distinguish inclusion cysts from simple cysts may have clinical impact and future larger scale studies should also evaluate quantitative methods of distinguishing these two types of cysts.

One of the drawbacks of OCT is that it requires close proximity to the tissue being imaged. OCT can be packaged into small (<1 mm) diameter probes and allows for potential applications in ultrasound (US) guided transvaginal imaging. This method of imaging is considerably less invasive than laparoscopy and could likely be performed with only mild sedation rather than general anesthesia. Although not within the scope of this pilot study, transvaginal OCT imaging may provide a screening tool for patients known to be high risk for ovarian cancer. Given the additional subsurface information it provides, it has potential for *in vivo* identification of suspicious lesions and guidance of small biopsy site acquisition in place of total ovary resection. US guided transvaginal OCT imaging may also be useful in the diagnosis of endometriosis, which currently requires laparoscopic visualization of endometrial implants outside the uterus for diagnosis. In this study, we were able to visualize endometrial implants and associated vascular changes with OCT and it is plausible that these criteria may also be applicable to other frequent locations for endometriosis, such as the broad ligament which may be accessed by transvaginal OCT. Future studies will aim to develop a transvaginal OCT probe and evaluate its abilities for ovarian imaging.

A major limitation of the study was the small patient number and specifically, the small number of benign and malignant neoplastic cases. However, given the preliminary investigative nature of this pilot study, the primary aim was to establish feasibility and safety of the imaging technique with a secondary goal of outlining microstructural features of each disease category. It is important that future larger scale *ex vivo* and *in vivo* studies address: 1) further qualitative evaluation of features to distinguish normal ovary, endometriosis, cystadenoma, borderline tumors, and adenocarcinoma, 2) the evaluation of malignant neoplasms of stromal and germ cell origin, 3) quantitative evaluation of features, such as stromal collagen orientation patterns of normal and neoplastic ovary or texture analysis of cyst linings to differentiate simple cysts from inclusion cysts and benign cystadenoma from borderline tumors and adenocarcinoma, and 4) evaluation of the sensitivity and specificity of these defined potentially diagnostic features. Additionally, as this study was a pilot study to qualitatively distinguish normal from pathologic ovarian tissue, the bilateral ovaries from a single patient were treated as independent; however, it should be recognized that in future, more quantitative evaluations of ovarian tissue, bilateral ovaries of a patient should not be treated as independent samples.

A second limitation to the study was the complexity of correlating *in vivo* OCT imaging sites with biopsy site selections following oophorectomy. Great attention was given to noting unique features seen laparoscopically (i.e. position with respect to fallopian tube and fimbriae) at each imaging site for maximal correspondence to biopsy sites. However, the ovary is symmetrical with few anatomical landmarks, thus this correlation was not always optimal. The use of marking inks, thermal damage marks, puncture sites, and/or suture was considered, but the application of any of these had potential to further complicate the imaging protocol by obscuring imaging sites, damaging biopsy sites/surgical specimens, and increasing anesthesia time. Obtaining the biopsy sites *in vivo* through laparoscopic ports was also considered, but has potential to increase the risk of intraoperative bleeding and would provide a more limited biopsy size than if obtained *ex vivo*. In future studies, the correlation between imaging sites and biopsy site selection may be improved with the laparoscopic application of a fine, precisely delivered marking ink adjacent to each imaging site subsequent to imaging to provide a method of correlation without obscuring or damaging the imaging site.

In this study, the development and successful implementation of the first laparoscopic OCT probe is presented. Comparison of OCT images and corresponding histopathology allowed for the description of preliminary microstructural features of normal ovary including epithelial inclusions cysts, endometriosis, and benign and malignant surface epithelial

neoplasms. Future *ex vivo* and *in vivo* studies will include larger patient numbers and evaluate a finer disease spectrum to develop more concrete qualitative and quantitative criteria to differentiate the normal ovary, benign cyst (simple and inclusion), cystadenoma, borderline tumors, and malignant neoplasms of epithelial, stromal, and germ cell origin. The fact that visual inspection of the images could be so well correlated with the pathology such that we could consistently differentiate normal ovary from serous cystadenoma, endometriosis and cancer is encouraging. Better quantitation of changes will be important to differentiate these entities which carry a very different prognosis and treatment plan. Future studies may also include ultrasound guided transvaginal imaging, dual modality imaging (combining OCT imaging with either spectroscopic or confocal imaging), and potentially volumetric ovarian imaging.

Supplementary Material

Refer to Web version on PubMed Central for supplementary material.

Acknowledgments

The authors would like to thank Dr. Urs Utzinger for his contributions to this study.

Reference List

1. Cancer Facts and Figures. American Cancer Society; 2008.
2. Badgwell D, Bast RC Jr. Early detection of ovarian cancer. Dis Markers. 2007; 23(5–6):397–410. [PubMed: 18057523]
3. Bast RC Jr, Brewer M, Zou C, Hernandez MA, Daley M, Ozols R, et al. Prevention and early detection of ovarian cancer: mission impossible? Recent Results Cancer Res. 2007; 174:91–100. [PubMed: 17302189]
4. Munkarah A, Chatterjee M, Tainsky MA. Update on ovarian cancer screening. Curr Opin Obstet Gynecol. 2007; 19(1):22–6. [PubMed: 17218847]
5. Nossov V, Amneus M, Su F, Lang J, Janco JM, Reddy ST, et al. The early detection of ovarian cancer: from traditional methods to proteomics. Can we really do better than serum CA-125? Am J Obstet Gynecol. 2008; 199(3):215–23. [PubMed: 18468571]
6. Partridge E, Kreimer AR, Greenlee RT, Williams C, Xu JL, Church TR, et al. Results From Four Rounds of Ovarian Cancer Screening in a Randomized Trial. Obstet Gynecol. 2009; 113(4):775–82. [PubMed: 19305319]
7. Kaku T, Ogawa S, Kawano Y, Ohishi Y, Kobayashi H, Hirakawa T, et al. Histological classification of ovarian cancer. Med Electron Microsc. 2003; 36(1):9–17. [PubMed: 12658347]
8. Kurman RJ, Shih I. Pathogenesis of ovarian cancer: lessons from morphology and molecular biology and their clinical implications. Int J Gynecol Pathol. 2008; 27(2):151–60. [PubMed: 18317228]
9. Drexler W. Cellular and functional optical coherence tomography of the human retina: the Cogan lecture. Invest Ophthalmol Vis Sci. 2008; 48(12):5339–51. [PubMed: 18055780]
10. Chen TC, Zeng A, Sun W, Mujat M, de Boer JF. Spectral domain optical coherence tomography and glaucoma. Int Ophthalmol Clin. 2008; 48(4):29–45. [PubMed: 18936635]
11. Testoni PA, Mangiavillano B. Optical coherence tomography in detection of dysplasia and cancer of the gastrointestinal tract and bilio-pancreatic ductal system. World J Gastroenterol. 2008; 14(42):6444–52. [PubMed: 19030194]
12. Suter MJ, Vakoc BJ, Yachimski PS, Shishkov M, Lauwers GY, Mino-Kenudson M, et al. Comprehensive microscopy of the esophagus in human patients with optical frequency domain imaging. Gastrointest Endosc. 2008; 68(4):745–53. [PubMed: 18926183]
13. Tearney GJ, Jang IK, Bouma BE. Optical coherence tomography for imaging the vulnerable plaque. J Biomed Opt. 2006; 11(2):021002. [PubMed: 16674177]

14. Guagliumi G, Sirbu V. Optical coherence tomography: high resolution intravascular imaging to evaluate vascular healing after coronary stenting. Catheter Cardiovasc Interv. 2008; 72(2):237–47. [PubMed: 18655155]
15. Boppart SA, Bouma BE, Pitris C, Tearney GJ, Fujimoto JG, Brezinski ME. Forward-imaging instruments for optical coherence tomography. Opt Lett. 1997; 22(21):1618–20. [PubMed: 18188315]
16. Boppart SA, Goodman A, Libus J, Pitris C, Jesser CA, Brezinski ME, et al. High resolution imaging of endometriosis and ovarian carcinoma with optical coherence tomography: feasibility for laparoscopic-based imaging. Br J Obstet Gynaecol. 1999; 106(10):1071–7. [PubMed: 10519434]
17. Brewer MA, Utzinger U, Barton JK, Hoying JB, Kirkpatrick ND, Brands WR, et al. Imaging of the ovary. Technol Cancer Res Treat. 2004; 3(6):617–27. [PubMed: 15560720]
18. Feldchtein FI, Gelinkonov GV, Gelinkonov VM, Kuranov RV, Sergeev AM, Gladkova ND, et al. Endoscopic applications of optical coherence tomography. Opt Express. 1998; 3:257–70. [PubMed: 19384368]
19. Escobar PF, Belinson JL, White A, Shakhova NM, Feldchtein FI, Kareta MV, et al. Diagnostic efficacy of optical coherence tomography in the management of preinvasive and invasive cancer of uterine cervix and vulva. Int J Gynecol Cancer. 2004; 14(3):470–4. [PubMed: 15228420]
20. Escobar PF, Rojas-Espaillat L, Tisci S, Enerson C, Brainard J, Smith J, et al. Optical coherence tomography as a diagnostic aid to visual inspection and colposcopy for preinvasive and invasive cancer of the uterine cervix. Int J Gynecol Cancer. 2006; 16(5):1815–22. [PubMed: 17009977]
21. Gossage KW, Tkaczyk TS, Rodriguez JJ, Barton JK. Texture analysis of optical coherence tomography images: feasibility for tissue classification. J Biomed Opt. 2003; 8(3):570–5. [PubMed: 12880366]
22. Pitris C, Goodman A, Boppart SA, Libus JJ, Fujimoto JG, Brezinski ME. High-resolution imaging of gynecologic neoplasms using optical coherence tomography. Obstet Gynecol. 1999; 93(1):135–9. [PubMed: 9916971]
23. Sergeev AM, Gelinkonov VM, Gelinkonov GV, Feldchtein FI, Kuranov RV, Gladkova ND, et al. In vivo endoscopic OCT imaging of pre-cancer and cancer states of human mucosa. Optics Express. 1997; 1(13):432–40. [PubMed: 19377567]
24. Zuluaga AF, Follen M, Boiko I, Malpica A, Richards-Kortum R. Optical coherence tomography: a pilot study of a new imaging technique for noninvasive examination of cervical tissue. Am J Obstet Gynecol. 2005; 193(1):83–8. [PubMed: 16021063]
25. Rollins AM, Kulkarni MD, Yazdanfar S, Ung-arunyawee R, Izatt JA. In vivo video rate optical coherence tomography. Opt Express. 1998; 3:219–29. [PubMed: 19384364]
26. Leeper K, Garcia R, Swisher E, Goff B, Greer B, Paley P. Pathologic findings in prophylactic oophorectomy specimens in high-risk women. Gynecol Oncol. 2002; 87(1):52–6. [PubMed: 12468342]
27. Lu KH, Garber JE, Cramer DW, Welch WR, Niloff J, Schrag D, et al. Occult ovarian tumors in women with BRCA1 or BRCA2 mutations undergoing prophylactic oophorectomy. J Clin Oncol. 2000; 18(14):2728–32. [PubMed: 10894872]
28. Powell CB, Kenley E, Chen LM, Crawford B, McLennan J, Zaloudek C, et al. Risk-reducing salpingo-oophorectomy in BRCA mutation carriers: role of serial sectioning in the detection of occult malignancy. J Clin Oncol. 2005; 23(1):127–32. [PubMed: 15625367]

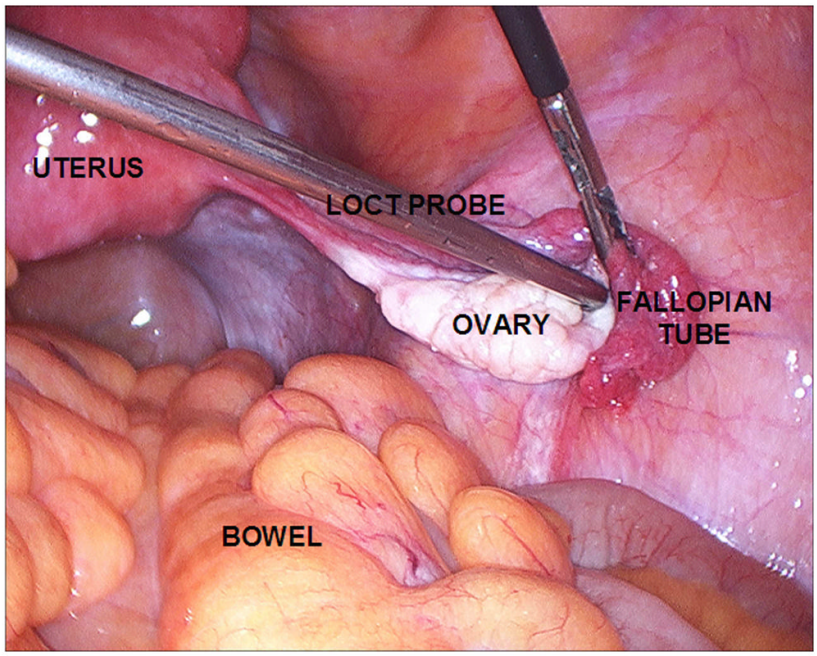

Figure 1.
Laparoscopic OCT during intraoperative use.

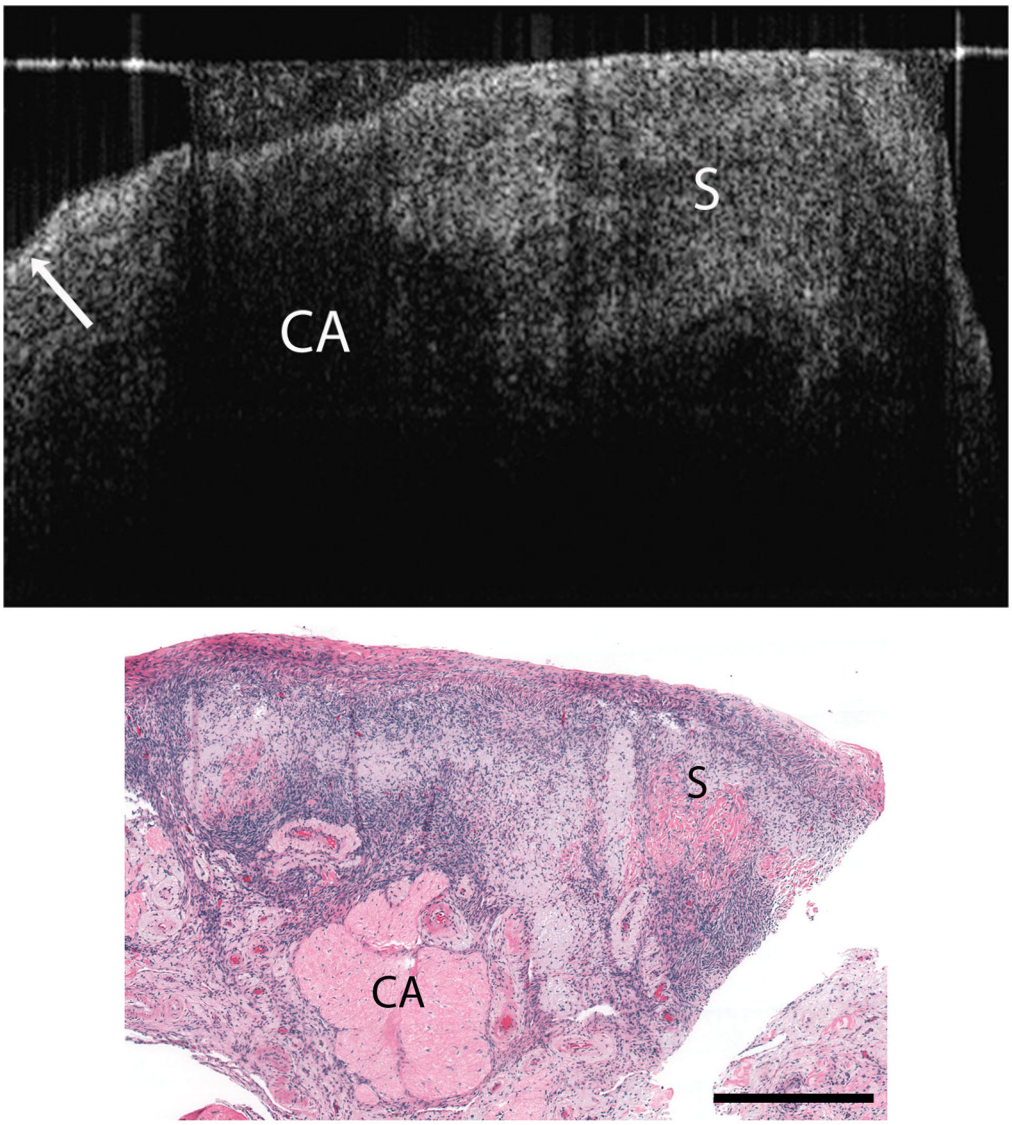

Figure 2. Normal post-menopausal ovary

(a) OCT of normal post-menopausal ovary (2.4 × 1.4 mm) with large corpus albicans and (b) corresponding histology. OCT and histopathology images are to scale. Scale bar, 500 μm. Arrow head: Surface epithelial backreflection, S: Stroma, CA: Corpus albicans.

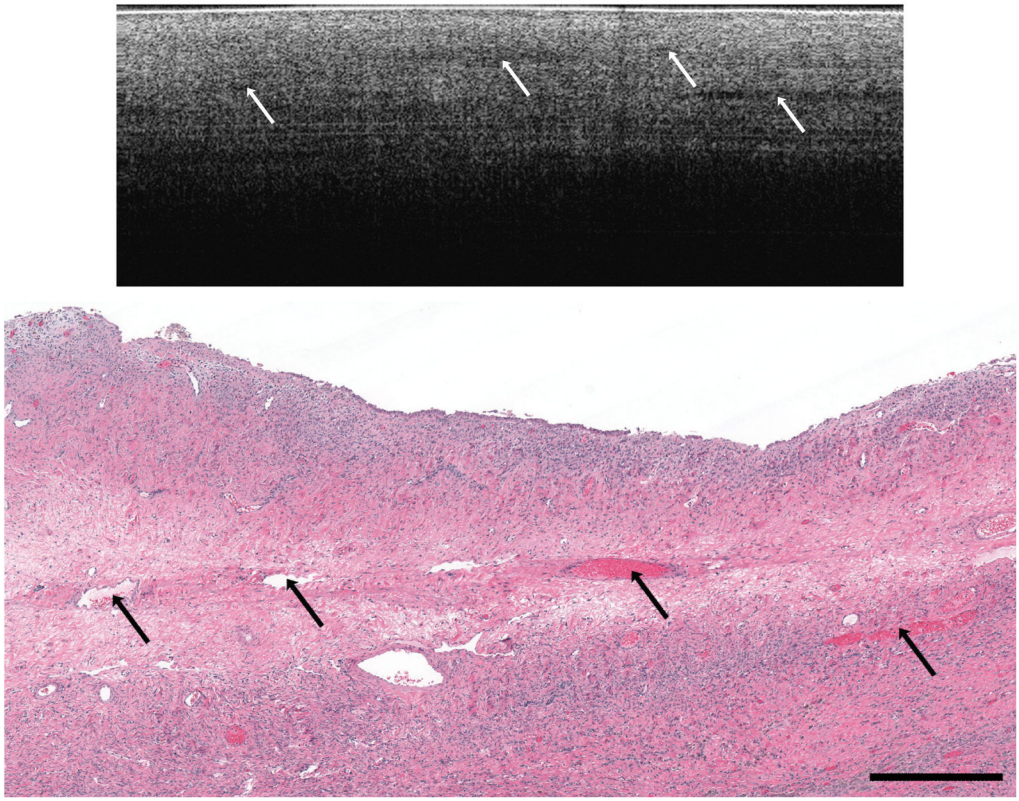

Figure 3. Endometriosis

(a) OCT image of ovarian stroma (4 × 1.4 mm) in endometriosis with increased vasculature and (b) corresponding histopathology. OCT and histopathology images are to scale. Scale bar, 500 μm. Arrows: Blood vessels.

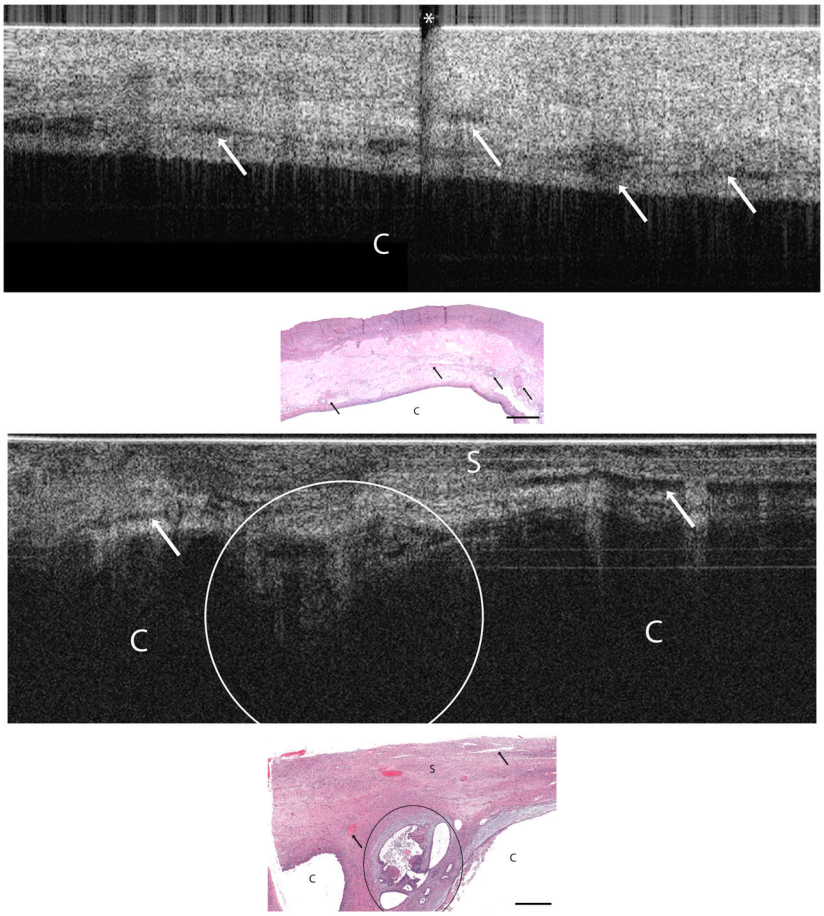

Figure 4. Serous cystadenoma and endometrioid adenocarcinoma

(a) OCT image of papillary serous cystadenoma (4 × 1.4 mm) and (b) corresponding histopathology. (c) OCT image of endometrioid adenocarcinoma (4 × 1.4 mm) and (d) corresponding histopathology. OCT and histopathology images are to scale. Scale bar, 500 μm. C: Cyst, Arrows: Blood vessels, S: Stroma, Circled region: Malignant glands, Asterisk: Imaging system artifact.